Resonant behaviour of the barrier of $YBa_2Cu_3O_7$ grain boundary Josephson junctions fabricated on bicrystalline substrates with different geometries

M.A. Navacerrada [a,*], M.L. Lucia [b], F. Sanchez-Quesada [b]

[a] Grupo de Acústica Arquitectónica, Escuela Técnica Superior de Arquitectura, Universidad Politécnica de Madrid, Avenida Juan de Herrera 4, 28040 Madrid, Spain
[b] Departamento Fisica Aplicada III (Electricidad y Electronica), Facultad de Cc. Fisicas, Universidad Complutense, Avenida Complutense s/n, 28040 Madrid, Spain

ARTICLE INFO

Article history:
Received 24 July 2012
Received in revised form 5 September 2012
Accepted 23 September 2012
Available online 29 September 2012

Keywords:
Proximity effects
Weak links
Tunneling phenomena
Josephson effects

ABSTRACT

We have analyzed a resonant behavior in the dielectric constant associated to the barrier of $YBa_2Cu_3O_7$ (YBCO) grain boundary Josephson junctions (GBJJs) fabricated on a wide variety of bicrystalline substrates: 12° [001] tilt asymmetric, 24° [001] tilt asymmetric, 24° [001] tilt symmetric, 24° [100] tilt asymmetric, 45° [100] tilt asymmetric and 24° [001] tilt symmetric +45° [100] tilt asymmetric bicrystals. The resonance analysis allows us to estimate a more appropriate value of the relative dielectric constant, and so a more adequate value for the length L of the normal N region assuming a SNINS model for the barrier. In this work, the L dependence on the critical current density Jc has been investigated. This analysis makes possible a single representation for all the substrate geometries independently on around which axes the rotation is produced to generate the grain boundary. On the other hand, no clear evidences exist on the origin of the resonance. The resonance frequency is in the order of 10^{11} Hz, pointing to a phonon dynamic influence on the resonance mechanism. Besides, its position is affected by the oxygen content of the barrier: a shift at low frequencies is observed when the misorientation angle increases.

1. Introduction

The transport and in general all the properties of $YBa_2Cu_3O_7$ (YBCO) weak links depend strongly on their structural quality. The physics taking place at YBCO surfaces and interfaces is rich, primarily because of phenomena associated with the d-wave order parameter symmetry [1]. All this has originated various hypotheses on the transport properties. The most widespread models are basically all in between two ideas: on the one hand resonant tunneling through some kind of dielectric barrier; on the other, especially in grain boundary Josephson junctions (GBJJs), a barrier composed of insulating regions separated by conducting channels, which act as shorts or micro bridges. These channels may have different sizes and distributions and obviously a different impact on the transport properties. Magnetoconductance measurements in YBCO GBJJs suggest that transport occurs in narrow channels up to 0.1 μm [2]. As a consequence a generic property in YBCO junctions appears to be a remarkably long life time of the carriers. This has been proved by optical and magnetoconductance measurements [3,4]. In any case, the barrier region is still hard to define, either in its spatial extent or its influence on the adjacent superconducting regions.

Also, in studies on artificially fabricated grain boundaries the observation that the critical current density Jc of a GBJJs depends exponentially on the misorientation angle has been made. A recent publication explores that the primary cause of this exponential dependence is the charging of the interface near defects which resemble classical dislocation cores. This leads to a porous barrier where weak links are distributed in a characteristic way depending on the misorientation angle. The d wave order parameter symmetry and the nature of the atomic wave functions at the boundary which modulate the hopping amplitudes do not appear to be essential for the functional form of the angle dependence [5].

In this work, we analyze the presence of a resonance response in YBCO GBJJs fabricated using different bicrystalline substrate geometries. The results derived offer a complementary analysis that allows us to corroborate the data already published on the spatial extension of the regions adjacent to the barrier. In fact, we show the adequacy of using the length L of the N region in a SNINS barrier instead of the misorientation bicrystal angle to plot the decrease of Jc in GBJJs. On the other hand, although caution is required, the range of the resonance frequency measured and its dependence position on the oxygen content of the barrier points to a phonon dynamic influence.

2. Experimental procedure

We have fabricated GBJJs based on YBCO of three different tilt geometries: [001] tilt, [001] tilt and [100] tilt. Josephson junctions were fabricated using $SrTiO_3$ (STO) bicrystalline substrates.

* Corresponding author. Tel.: +34 91 336 42 48; fax: +34 91 336 65 54.
E-mail address: mdelosangeles.navacerrada@upm.es (M.A. Navacerrada).

We have chosen 12° [001] asymmetric, 24° [001] symmetric and 24° [001] asymmetric bicrystalline substrates of STO as [001] tilt geometries, 24° [100] asymmetric and 45° [100] asymmetric substrates to fabricate the [100] tilt junctions and as well 24° [001] symmetric +45° [100] asymmetric STO bicrystals as one [100] tilt tilt geometry. The scheme of Fig. 1 illustrates the different tilt bicrystalline substrates: the misorientation angles for all the geometrical configurations are indicated in Table 1. The [100] tilt and [100] tilt-tilt bicrystal geometries are of the "valley" type where the [001] axis is tilted towards the grain boundary.

The bicrystal technique is the most direct way to create a grain boundary. This is an easy way to vary the relative orientations of the electrodes in different possible combinations. Other approaches, as step, step-edge and biepitaxial techniques are more flexible in the location of the junctions for fundamental studies and more efficient for circuit design, but the GBJJs are limited to particular misorientation angles, and the performances of some of these junctions may be less reliable. The bicrystal techniques have been by far the most used, in part because of its simplicity and extendibility to any other high temperature superconductor compounds and deposition techniques [1].

YBCO films were epitaxial grown in a high pressure (3.4 mbar) pure oxygen dc sputtering system. In the deposition process the substrate temperature was 900 °C. The accurate control of the film growth process in our sputtering system has been previously demonstrated [6,7]. Films were patterned obtaining junctions widths (W) ranging between 2 and 20 μm for all the STO bicrystals by Ar ion milling. 100 nm thick gold layers were deposited on the samples for making low contact resistance paths.

The current voltage, I–V, curves of the samples have been measured using a homemade electronics set-up characterized by a current amplifier showing 0.1 nA/Hz$^{1/2}$ current noise and a voltage differential amplifier with 7 nV/Hz$^{1/2}$ output voltage noise at 10 Hz. Moreover, the junction leads are filtered by individuals cryogenic π filters (one filter per wire), located close to the sample with a cut off frequency of about 10 kHz. This guarantees that no high-frequency contribution (rf signals) coming from the external environment is reaching the junctions.

3. Results and discussion

We have observed Fiske steps in all the YBCO GBJJs fabricated on the different bicrystalline geometries. Several plots of the evidence of the presence of Fiske steps in the I–V curves have been published in references [6,8,9]. Examples of I–V curves corresponding to some of the bicrystalline geometries analyzed have been plotted in Fig. 2 for values of the magnetic field for which the Fiske steps are clearly observed. No doubts arise in their identification since the dependence of their intensity on the magnetic field is as predicted by theory [10].

In general, the structural and electrical information about the barrier has been mainly derived from the transport parameters:

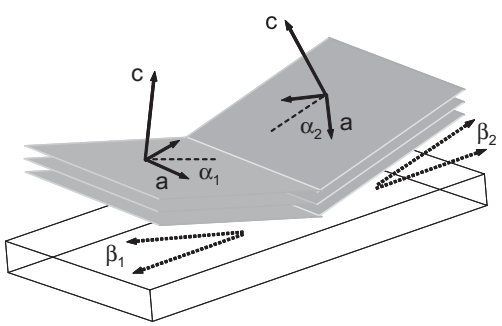

Fig. 1. Schematic representation of the [001] and [100] bicrystal orientations.

normal resistance (R_N) and critical current (I_C). However, we have already shown the usefulness of the information that can be obtained from the analysis of these resonances [6,8,9,11]. This fact was also pointed out by Tafury et al.: the resistance of the barrier was derived from the voltage displacement induced by irradiation on the resonance steps [12].

In this line, the presence of these resonances allows us to analyze the dielectric response of the barrier. The Swihart velocity $\bar{c}$ is determined by the voltage position of the Fiske step $n = 1$ by means of the expression $V_1 = \frac{\phi_0 \bar{c}}{2W}$ where W is the junction width and ϕ_0 the magnetic flux quantum [13]. The ratio of the dielectric constant to the thickness of the barrier $\frac{\varepsilon}{t}$ is calculated using $\bar{c} = \left[c_0 \left(\frac{t}{\varepsilon d}\right)^{1/2}\right]$ where c_0 is the vacuum light velocity and d the effective magnetic junction length. At this point, it is necessary to guarantee that the external circuit does not influence the $\frac{\varepsilon}{t}$ calculated values. Considering the extremely low values of the junctions capacitances (of the order of several femtofarads) and in order to guarantee that the external circuit does not influence the measurements, the effect of stray capacitances and/or inductance of wire connecting the junctions pads to the cryogenic filters is also worthy to be analyzed. As a rough calculation, the resonance frequency related to the external circuit is of the order of 30 MHz. If the total capacitance of the circuit would be the one associated with the wires, this would induce a current step in the I–V curve at the voltage $V \approx 2\mu V$ that is lower than the range we are dealing with [11]. It means that the capacitance we have measured by using current steps is completely due to the junction.

Returning to the calculus, form the Fiske voltage position the resonance frequency of the cavity can also be determined by means of the expression $f_1 = \frac{V_1}{\phi_0}$ [10]. Following this procedure, the $\frac{\varepsilon}{t}$ ratio and the f_1 values have been calculated for each substrate geometry and for W values ranging between 2 and 20 μm. Then, we have established a relation $\varepsilon(f_1)$ which is essentially the dispersion relation $\varepsilon(\omega)$. In the articles published in the literature focusing in the $\frac{\varepsilon}{t}$ ratio of [001] tilt junctions a single average value of such parameter is given for all the junctions independently of W [12,14–16].

In all the bicrystalline geometries fabricated a resonant behaviour is detected. In this sense the data has been fitted to the dispersion relation [17]:

$$\varepsilon = \varepsilon_0 + \frac{NQ^2}{m} \frac{\omega_0^2 - \omega^2}{(\omega_0^2 - \omega^2)^2 + 4\gamma^2\omega^2} \tag{1}$$

where ε_0 is the vacuum dielectric constant, N the number of atoms per volume unit, Q the charge carrier per unit cell, m the mass of free electrons and γ the damping constant. In the fitting $\frac{NQ^2}{m}$, ω_0 and γ have been considered as free parameters. Also for the fitting a t value has had to be considered in order to deduce the ε values from the experimental $\frac{\varepsilon}{t}$ ratios. It has been published a phenomenological criterion to estimate the thickness of the nonsuperconducting layer enveloping the grain boundary if the distribution of the strain in its vicinity is known. This criterion suggests that cores of the dislocations are no transparent for the supercurrent because the superconductivity is suppressed in the region of the crystal lattice where strains achieve some critical values [18]. Applying this approach and based on that the suppression of the superconductivity by strain is caused by the change of the bond lengths, the valence of atoms and the number of charge carriers present in the grain boundary structure the distribution of the strain in the vicinity of the grain boundary is determined. According to this model the width of the nonsuperconducting zone has been estimated to be 1–3 nm depending on the orientation angle and geometry of the grain boundary [19]. In this line, we have considered correct to use a value of 1 nm for the 12° [001] geometry and 2 nm for the others bicrystalline geometries.

Table 1
Values of the bicrystal α and β misorientation angles.

Bicrystal geometry	$\alpha_1(^\circ)$	$\alpha_2(^\circ)$	$\beta_1(^\circ)$	$\beta_2(^\circ)$
[001] tilt: 12° [001] asymmetric	0	12	0	0
[001] tilt: 24° [001] symmetric	12	12	0	0
[001] tilt: 24° [001] asymmetric	0	24	0	0
[100] tilt: 24° [100] asymmetric	0	0	0	24
[100] tilt: 45° [100] asymmetric	0	0	0	45
[100] tilt–tilt: 24° [001] symmetric + 45° [100] asymmetric	12	12	0	45

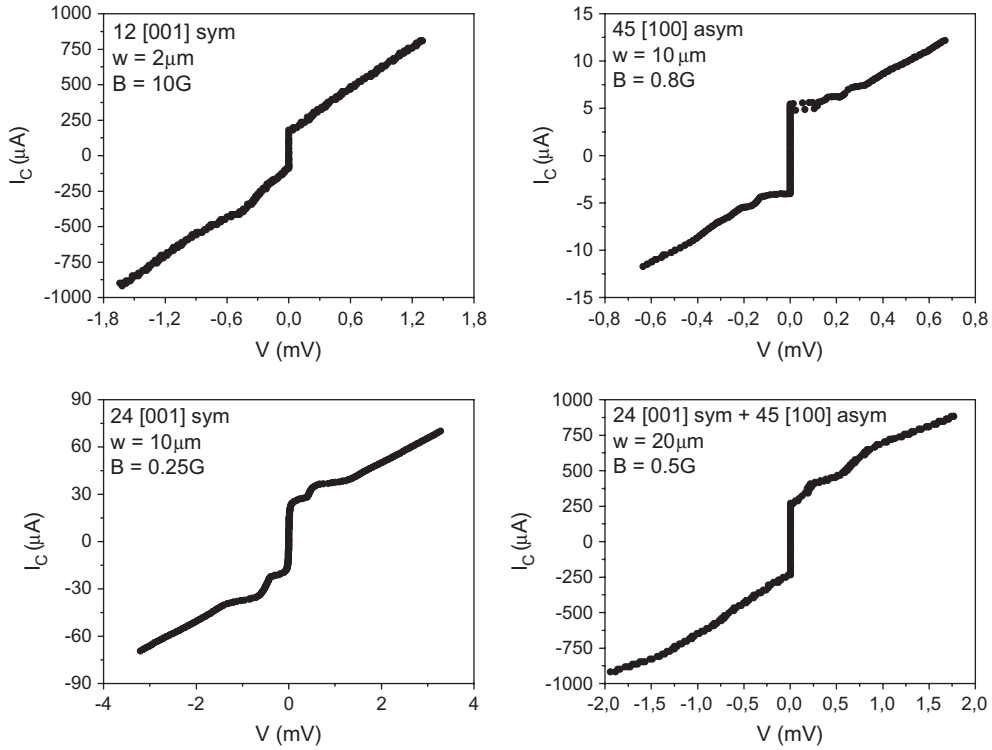

Fig. 2. Examples of *I–V* curves corresponding to some of the bicrystalline geometries analyzed for a fixed value of the magnetic field indicated in each plot.

Table 2
Values of ω_0 and γ (expressed in Hz and cm^{-1}) deduced by the fitting to expression (1).

Bicrystalline geometry	ω_0 ($\times 10^{11}$ Hz cm^{-1})	γ ($\times 10^{10}$ Hz cm^{-1})
12° [001] asymmetric	7.5–25.2	3.9–1.3
24° [001] symmetric	4.4–14.7	1.7–0.6
24° [001] asymmetric	4.2–14	1.1–0.5
24° [100] asymmetric	7.4–24.7	6.0–2.0
45° [100] asymmetric	3.3–11	2.0–0.7
24° [001] symmetric +45° [100] asymmetric	2.9–9.7	2.2–0.8

In Table 2 we have quoted the values obtained for ω_0 and γ for all the bicrystalline geometries. The resonance frequency varies between 7 and 2×10^{11} Hz depending on the substrate geometry. Some aspects related to the nature and transport mechanism of the YBCO GBJJs can be deduced and corroborated from its analysis.

In several published works [6,20], values of the relative dielectric constant ε_r' ranging between 5 and 10 have been assumed for the barrier from the estimation of oxygen deficient YBCO [21]. At this point, a more appropriate value of the relative dielectric constant associated to the barrier is the low frequency relative dielectric constant given by the expression:

$$\varepsilon_r' = 1 + \frac{NQ^2}{m\varepsilon_0\omega_0^2} \tag{2}$$

where the ratio $\frac{NQ^2}{m}$ and the ω_0 values are derived from the fitting to expression (1). This approximation allows us to calculate a ε_r' value for each geometry that correctly considers its particular barrier microstructure. The obtained values have been shown in Table 3. Also, an experimental estimation of t can be made from the $\frac{e}{t}$ ratios. The range of t values is indicated in Table 3.

Previously the dependence of the critical current on the junction resistance has been investigated pointing to a description of the barrier as a SNINS structure [22]. Assuming that the resonance observed is associated to the insulating I region, the length L of the normal N region has been estimated from the discrepancy observed in the capacitance values derived from the Fiske resonance voltage positions and the *I–V* curve hysteresis. In the calculus we have used the ε_r' values derived from expression (2) and shown in Table 3. A detailed explanation of this calculus has been published in Refs. [6,9].

The L values calculated are in the interval indicated in Table 3. We believe that the wide interval for the L values in some geometry is a consequence of the faceting of the barrier. On the other hand, the magnitude of such values for some geometries may seem strange. However, these values derived from the resonant behaviour of the barrier confirm other results already published in the literature. Techniques as the strain analysis [23] and the atomic force microscopy [19] reveal that meandering widths range from 5 to 100 nm in [100] tilt junctions.

As we have mentioned in the introduction, different works emphasize that the transport properties of the grain boundary Josephson junctions strongly depend on the misorientation angle between the two electrodes. In particular, in artificially grain boundaries it has been observed that the critical current Jc of GBJJs depends exponentially on the misorientation angle [5]. Common usage distinguishes the symmetric case, in which the misorientation between the crystalline axes and the junction interface is the same on the two sides of the junction, from the asymmetric case, in which this misorientation is zero on one side of the interface. In this line, it has been found that in the low angle regime (010) tilt boundaries and (100) twist boundaries reduce the critical current density much less than (001) tilt boundaries with the same misorientation angle. Transmission electron microscopy reveals a low defect density in the (010) tilt boundaries [24]. We have analyzed the dependence of Jc on the geometry in our junctions. However, we have chosen L for the plot. We consider this parameter more adequate for such a representation because it is not necessary to distinguish between different geometries with the same misorientation angle, so it allows a single representation for all the geometries independently on around which axis the rotation is produced to generate the grain boundary. The results have been plotted in Fig. 3. The Jc values are in the order of magnitude of the values reported in the literature for junctions of the same thickness and bicrystalline geometries.

Coming into the analysis of the fitting of Fig. 3, two different regions can be appreciated approximately limited by a length L ranging between 30 and 40 nm. For values of L smaller than 40 nm the data fit well to an exponential expression on L of the type $Jc = Ae^{-\frac{L}{L_0}}$ as indicated by the solid line. From such a fitting, the values derived from A and L_0 have been 0.92×10^6 A/cm^2 and 6.4 nm respectively. The values obtained for both parameters seem reasonable. For example, following the exponential expression the A value would correspond to a junction with $L = 0$, so to a thin film or to a grain boundary of low angle of misorientation. In this sense, the A value is close to the value of an YBCO thin film of high quality at 77 K.

For L values up to around 30–40 nm, the channel model can be useful in describing the transport properties of the barrier: an inhomogeneous barrier with a large number of conducting parallel channels that support the current. We believe that this model is supported by the behaviour shown in Fig. 3. The number of superconducting channels, and so Jc, must be severely dependent on the width of the GBJJs and so, on the L value. For low angles boundaries (up to 24) even in the case of (010) tilt boundaries and (100) twist boundaries, it has been demonstrated that the model of dependence on the misorientation angle works. For these angles, the presence of uninterrupted YBCO unit cell planes has been confirmed [24].

However, when L is above 40 nm, the Jc dependence on this parameter is weak, for L values ranging between 60 and 100 nm the Jc values are almost constant. This behaviour seems reasonable: when L reaches a length above 60 nm the number of filaments in the barrier must decrease drastically and so, be independent on the bicrystalline geometry.

Table 3
Values of ε_r' and intervals of values for t and L.

Bicrystalline geometry	ε_r'	t (nm)	L (nm)
12° [001] asymmetric	18	(0.2–0.8)	(0–0.7)
24° [001] symmetric	28	(0.4–1.2)	(0–2)
24° [001] asymmetric	26	(0.7–1.6)	(0–2)
24° [100] asymmetric	20	(0.6–2)	(0–1)
45° [100] asymmetric	37	(0.7–3.6)	(5–26)
24° [001] symmetric +45° [100] asymmetric	43	(0.8–2.5)	(31–110)

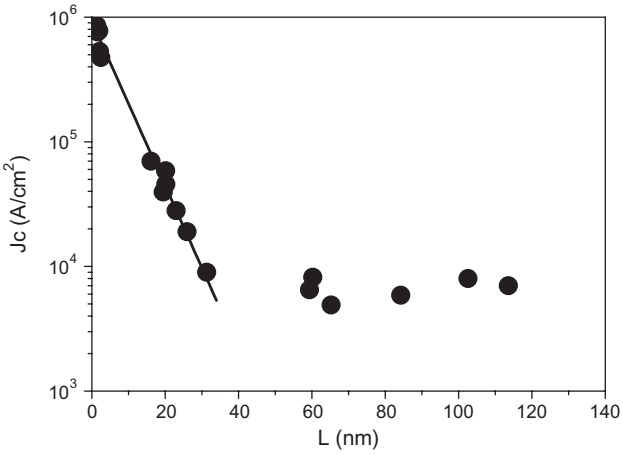

Fig. 3. Jc versus L, the length of the normal region following a SNINS model for the barrier. The solid line corresponds to the fitting to the exponential expression $Jc = Ae^{-\frac{L}{L_0}}$.

On the other hand, for this L range different transport mechanism scenarios could be possible. In (100) tilt junctions it seems that the dielectric barrier contains a high density of localized states and the quasiparticle and Cooper pairs current is dominated by resonant tunnelling via these localized states. If many impurities are present, the bound states overlap and interfere leading to the band analogous to the impurity band in disordered semiconductors [25]. Regarding these results a mixed picture of the barrier could be more reasonable for the bicrystalline geometries in which L is higher than 20 nm: a barrier where a tunnelling transport via localized states is combined with a transport mechanism across superconducting filaments.

Up to our knowledge, in the literature the parameter that is always used for the plot of the decrease of Jc is the misorientation angle. Then, it is not possible to include directly data from other authors in Fig. 3 since no data of L values are available. Few references discuss about both methods of calculus of the capacitance associated to the barrier. In an analysis of the effect of the substrate on the dielectric properties of the barrier Tarte et al. [26] found that the capacitance obtained from the Fiske resonance correlates well with that determined from the hysteresis measurements on YBCO 24° and 36° [001] symmetrical GBJJs fabricated on STO bicrystal substrates. In accordance with this result, for the first geometry, we have shown small L values (see Table 3).

However, following with the comparison to other authors, we believe that the correlation observed between the capacitance per unit area (A) associated to the barrier (C/A) and the product R_NA confirms at least partially our results. Most data of YBCO junctions fabricated on different substrates and the 24° (001) tilt geometry fell close to a power law of the form $\frac{C}{A}\alpha(R_NA)^{-1}$ [26,27]. Our data relative to 24° [001] symmetric GBJJs follow this scaling behaviour with experimental data dispersion comparable to that reported in the literature [6]. This scaling behaviour is presented as consistent with the phenomenological filamentary model as the tendency plotted in Fig. 3 [28,29] for L values smaller than 40 nm. In the case of 45° [100] asymmetric GBJJs the C/A data calculated from Fiske steps present the opposite behaviour: the C/A ratio increases when R_NA increases [6]. As deduced from the tendency observed in Fig. 3 for L values up to 40 nm, a different structure of the barrier and transport mechanism is necessary to explain this bicrystalline geometry.

Concerning the origin of the resonance observed, the data available leads us to speculate on an optical phonon dynamic influence on the resonance mechanism. Assuming the SNINS model, we believe that the $\frac{\varepsilon}{t}$ ratio calculated from Fiske steps is only related to

the resonant cavity close to the crystallographic grain boundary, so the *I* region [11]. Such region is generally a very disordered region, strained, poor in oxygen and where the growth of impurities is favoured. So, from the structural characteristics of the barrier region it seems reasonable that the phonon structure becomes more pronounced than the electronic background, reinforcing the phononic nature of the resonance.

Different experimental techniques as Raman spectroscopy [30,31] or reflectivity measurements [32] have been used to investigate the optical phonon modes, oxygen contents and structural properties of YBCO thin films and single crystals. For YBCO the Raman phonon lines correspond to lattice vibrational modes involving motions of mainly one type of atoms and in general, five Raman modes whose position ranges between 502 cm^{-1} and 115 cm^{-1} have been established. In Table 2 the values of ω_0 have been also expressed in cm^{-1}: the resonance frequency position deduced from the fitting is lower than the frequency of any of the modes measured by Raman spectroscopy for full oxygenated samples. However, the oxygen sub-lattice related vibrations are very sensitive to YBCO stoichiometry and changes in the Raman spectra with the oxygen content have been also described [30,31]. The lines which are quite sharp in the highly doped material display several unusual properties as the oxygen content is reduced. The origin of many additional spectral features most strongly pronounced in poorly oxygenated, doped or mixed YBCO samples, is either unclear or controversially discussed. Nevertheless, there is a general agreement that the presence of new bands is generally an indication of defects and local changes of the atomic environments.

Coming to our experimental results, we believe that the origin of the resonance we observe is the same for all the geometries. The resonance appears at a frequency of around 25 cm^{-1} for the 12° [001] and 24° [100] bicrystalline geometries. In the other geometries, this resonance is shifted to smaller frequencies ranging between 14 and 10 cm^{-1} depending on the geometry. Strain and oxygen deficiency at the barrier increase when the misorientation angle increases and the bicrystalline geometry is more complicated. Besides the frequency is almost coincident for the 24 ° [001] and 45° [100] geometries: it seems that rotation around [100] axis generates a lower lattice distortion than around the [001] axis.

In this line, independently on the association of the resonance to a known or new phonon band, its position is affected by the structure of the barrier. The shift to low frequencies of the resonance goes along with a decrease of the damping constant. These results are also reported by Schützmann et al. [32]. Few references related to Raman spectroscopy at grain boundaries have been found in the literature [33]. But a similar scenario has been detected by other authors. Admittance Josephson spectroscopy experiments on (100) tilt YBCO bicrystal junctions reveal the presence of additional lines whose localization is modified by oxygen annealing of the junctions [34].

4. Conclusions

We have shown that the barrier of all our GBJJs can be modelled as a dielectric medium with losses. Our data $\varepsilon(f_1)$ can be fitted to an expression $\varepsilon(\omega)$ that describes the behaviour of ε close to a resonance in a dielectric medium. The presence of the resonance allows us to calculate the width, *L*, of the normal *N* regions of a SNINS barrier using a different value for the dielectric constant for this region depending on the junction geometry. Jc is plotted as a function of the *L* values. Using this length it is not necessary to distinguish between different geometries with the same misorientation angle. In such a representation two transport regimes, already described in the literature, have been observed. The origin of this resonance seems to be the same for all the bicrystalline geometries studied and its position is affected by the structure of the barrier (oxygen order, strain, etc.). We speculate on a fundamentally phononic origin of this resonance.

References

[1] F. Tafuri, J.R. Kirtley, Weak links in high critical temperature superconductors, Rep. Prog. Phys. 68 (2005) 2573–2663.

[2] A. Tagliacozzo, F. Tafuri, E. Gambale, B. Jouault, D. Born, P. Lucignano, D. Stornaiuolo, F. Lombardi, A. Barone, B.L. Altshuler, Mesoscopic conductance fluctuations in $YBa_2Cu_3O_{7-x}$grain boundary junctions at low temperature, Phys. Rev. B 79 (1–10) (2009) 024501.

[3] N. Gedik, J. Orenstein, R. Liang, D.A. Bonn, W.N. Hardy, Diffusion of non-equilibrium quasi-particles in a cuprate superconductor, Science 300 (2003) 1410–1412.

[4] T. Bauch, T. Lindstrom, F. Tafuri, G. Rotoli, P. Delsing, T. Claeson, F. Lombardi, Quantum dynamics of a *d*-wave Josephson junctions, Science 311 (2006) 57–60.

[5] S. Grasser, P.J. Hirschfeld, T. Jopp, R. Gustser, B.M. Andersen, J. Mannhart, How grain boundaries limit the supercurrent in high temperature superconductors, Nat. Phys. 6 (2010) 609–614.

[6] M.A. Navacerrada, M.L. Lucía, L.L. Sánchez-Soto, F. Sánchez-Quesada, G. Testa, E. Sarnelli, Capacitance of Josephson junctions made on bicrystalline substrates of different geometries, Phys. Rev. B 71 (1–6) (2006) 014501.

[7] E. Sarnelli, G. Testa, D. Crimaldi, A. Monaco, M.A. Navacerrada, A class of high Tc $YBa_2Cu_3O_{7-x}$ grain boundary junctions with I_CR_N products, Supercond. Sci. Technol. (Rapid Commun.) 18 (2005) 35–39.

[8] M.A. Navacerrada, M.L. Lucía, L.L. Sánchez-Soto, F. Sánchez-Quesada, G. Testa, E. Sarnelli, Dispersion relation of the dielectric constant of $YBa_2Cu_3O_{7-x}$ grain boundary Josephson junctions tilted around different axes, IEEE Trans. Appl. Supercond. 17 (2007) 3541–3544.

[9] M.A. Navacerrada, M.L. Lucía, L.L. Sánchez-Quesada, E. Sarnelli, C. Nappi, Frequency analysis of the dielectric constant of $YBa_2Cu_3O_{7-x}$ Josephson junctions fabricated on bicrystalline substrates, Phys. Rev. B 74 (1–4) (2006) 024507.

[10] A. Barone, G. Paterno, Physics and Applications of the Josephson Effect, Wiley, New York, 1982.

[11] M.A. Navacerrada, M.L. Lucía, F. Sánchez-Quesada, E. Sarnelli, Fiske steps and hysteresis in $YBa_2Cu_3O_{7-x}$ grain boundary Josephson junctions: structural information of the barrier by means of a nondestructive approach, J. Appl. Phys. 104 (1–6) (2008) 113915.

[12] F. Tafuri, B. Nadgomy, S. Shokhor, M. Gurvitch, F. Lombardi, F. Carillo, A.DiChiara.E. Sarnelli, Barrier properties in $YBa_2Cu_3O_{7-x}$ grain-boundary Josephson junctions using electron-beam irradiation, Phys. Rev. B (Rapid Commun.) 57 (1-4) (1998) R14076.

[13] M.D. Fiske, Temperature and magnetic field dependences of the Josephson tunneling current, Rev. Mod. Phys. 36 (1964) 221–222.

[14] D. Winkler, Y.M. Zhang, P.A. Nilsson, E.A. Stepantsov, T. Claeson, Electromagnetic properties at the grain boundary interface of a $YBa_2Cu_3O_{7-x}$ bicrystal Josephson junctions, Phys. Rev. Lett. 72 (1994) 1260–1263.

[15] J.H.T. Ransley, P.F. McBrien, G. Burnell, E.J. Tarte, J.E. Evetts, R. Schulz, C.W. Scheneider, A- Schmehl, H. Bielefeldt, H. Hilgenkamp, J. Mannhart, Capacitance measurements on grain boundaries in $Y_{1-x}Ca_xBa_2Cu_3O_{7-x}$ bicrystal Josephson junction, Phys. Rev. Lett. 70 (1–11) (2004) 104502.

[16] E.J. Tarte, P.F. McBrien, J.H.T. Ransley, R.H. Hadfield, E.I. Inglessi, W.E. Booij, G. Burnell, M.G. Blamire, J.E. Evetts, Capacitance as a probe of high angle grain boundary transport in oxide superconductors, IEEE Trans. Appl. Supercond. 11 (2001) 418–421.

[17] H. Frohlich, Theory of Dielectrics, Oxford University Press, 1968.

[18] M.F. Chisholm, S.J. Pennycook, Structural origin of reduced critical currents at $YBa_2Cu_3O_{7-x}$ grain boundaries, Nature 351 (1991) 47–49.

[19] V.S. Boyko, A.M. Levine, Atomic structure of large-angle grain boundaries $\sum 5$ and $\sum 13$ in $YBa_2Cu_3O_7$ and their transport properties, Phys. Rev. B 64 (1–6) (2001) 224525.

[20] H. Hilgenkamp, J. Mannhart, Mechanisms controlling interface-properties in high T_c superconductors, IEEE Trans. Appl. Supercond. 9 (1999) 3405–3408.

[21] J. Humlicek, J. Kircher, H.U. Habermeier, M. Cardona, A. Roseler, Infrared optical response of $YBa_2Cu_3O_7$ and $PrBaCu_3O_7$ An ellipsometric study, Physica C 190 (1992) 383–395.

[22] M.A. Navacerrada, M.L. Lucía, F. Sánchez-Quesada, E. Sarnelli, Structural image of the barrier of $YBa_2Cu_3O_7$ grain boundary Josephson junctions based on the analysis of the electromagnetic parameters, IEEE Trans. Appl. Supercond. 19 (2009) 2863–2866.

[23] V.S. Boyko, Siu-Wai Chan, M. Chopra, Shape of a twin as related to the inelastic forces acting on twinning dislocations in $YBa_2Cu_3O_7$, Phys. Rev. B 63 (1–8) (2001) 224521.

[24] R. Held, C.W. Schneider, J. Mannhart, L.F. Allard, K.L. More, A. Goyal, Low angle grain boundaries in $YBa_2Cu_3O_7$ with high critical current densities, Phys. Rev. B 79 (1–7) (2009) 014515.

[25] H. Allou, J. Bobroff, M. Gabay, P.J. Hirschfeld, Defects in correlated metals and superconductors, Rev. Mod. Phys. 81 (2008) 45–108.

[26] P.F. McBrien, R.H. Hadfield, W.E. Booij, A. Moya, F. Kahlmann, M.G. Blamire, C.M. Pregum, E.J. Tarte, The capacitance of grain boundaries in

superconducting films with strontium titanate and other substrates, Physica C 339 (2000) 88–92. references therein.
[27] B.H. Moeckly, R.A. Buhrman, Electromagnetic properties of $YBa_2Cu_3O_{7-x}$ thin film grain boundary weak links, IEEE Trans. Appl. Supercond. 5 (1995) 3414–3417.
[28] H. Moeckly, D.K. Lathrop, R.A. Buhrman, Electromigration study of oxygen disorder and grain boundary effects in $YBa_2Cu_3O_{7-x}$ grain boundaries, Phys. Rev. B 47 (1993) 400–417.
[29] E. Sarnelli, P. Chaudhari, J. Lacey, Residual critical current in high T_c bicrystal grain boundary junctions, Appl. Phys. Lett. 62 (1993) 777–779.
[30] O. Martínez, J. Jiménez, P. Martín, A.C. Prieto, S. Degoy, D. Chambonnet, C. Belouet, S. Nicoletti, L. Correra, A microRaman study of the structural properties of PLD high T_c superconducting thin films, Physica C 270 (1996) 144–153.
[31] S. Hong, H. Jo, H. Cheong, G. Park, Characterization of defect modes in $YBa_2Cu_3O_7$ thin films probed by Raman scattering, Physica C 418 (2005) 28–34.
[32] J. Schützmann, S. Tajima, S. Miyamoto, Y. Sato, R. Hauff, Doping and temperature dependence of *c*-axis optical phonon in $YBa_2Cu_3O_y$ single crystals, Phys. Rev. B 52 (18) (2005) 13665–13673.
[33] I. Yang, B. Chang, G.Y. Sun, Raman study of the 90° grain boundaries $YBa_2Cu_3O_7$ thin films, Physica C 311 (1998) 75–80.
[34] Y. Divin, M. Lyatti, Josephson spectroscopy of terahertz losses in (100)-tilt YBCO bicrystal junctions, J. Phys.: Conf. Ser. 97 (2008) 012223.